Desalination and Water Treatment
www.deswater.com

doi: 10.5004/dwt.2019.24016

152 (2019) 268–275
June

Removal of aspartame by catalytic ozonation with nano-TiO_2 coated pumice

Alper Alver*, Emine Basturk

Department of Environmental Engineering, Engineering Faculty, Aksaray University, 68100 Aksaray, Turkey, Tel. +90 382 288 3630; emails: alperalver@gmail.com (A. Alver), eminebasturk@hotmail.com (E. Basturk)

Received 15 November 2018; Accepted 24 February 2019

ABSTRACT

Aspartame is widely used as an artificial sweetener and has been ubiquitously detected in various water sources, it is unstable and can produce some harmful degradation products under certain storage conditions. In this study, the degradation of aspartame through adsorption, single ozone, and catalytic ozonation was investigated. In order to create an eco-friendly catalyst, pumice surface was covered with nano-TiO_2 and physicochemical surface properties of the catalyst were systematically investigated by SEM, EDX, FT-IR, BET, DLS, and pH_{PZC} analysis. It was proved by SEM and EDX analysis that the nanostructures were homogeneously dispersed onto the catalyst surface and the surface of the catalyst was enriched at 5.5% by weight relative to the uncoated state. After coating, the catalyst surface area expanded by about 10 times and the pore diameters from 0.008 to 0.044. After characterization studies, the role of sole adsorption and sole ozonation in catalytic ozonation has been tried to be determined by using different doses of aspartame, catalyst, and ozone. In the catalytic ozonation experiments, reaction kinetics were analyzed in the presence of tert-butyl alcohol (TBA) that is a radical scavenger, and it was confirmed that the activity of •OH radicals increased after using n-TCP as a catalyst. The results demonstrated that sole ozonation and adsorption of aspartame was not effective for removal. The rate of removal increased significantly with combining adsorption and ozonation. Synergism percentage was calculated to be 91.53. The benefit of surface adsorption, hydroxyl radicals, and sole ozonation to catalytic ozonation was determined as 2.96%, 72.20%, and 24.84%, respectively. Although ozonation of aspartame was initiated by •OH radical, both $•OH^-$ radical and O_3 might be involved in the aspartame removal.

Keywords: Aspartame; Artificial sweetener; Catalytic ozonation; Sole ozonation; Adsorption; Nano-titanium dioxide; Synergism; Kinetics

1. Introduction

Aspartame, known as a highly addictive artificial sweetener and flavor enhancer, was discovered by James M. Schlatter in 1965 and has long been a subject of credibility after its ratification in the United States in 1974 [1]. Aspartame is used in over 10,000 products worldwide and a non-nutritive and low caloric sweetener which is approximately 180–200 times sweeter than artificial sweeteners such as sucrose [2]. Aspartame consists of aspartic acid, phenylalanine, and methanol. These substances commonly occur at various foods. The three forms of aspartame have neurotoxic effects on the human body [3]. In addition, artificial sweeteners are considered emerging contaminants in environmental sciences recently because it causes brain tumor and liver cancer [4]. The tendency about the fate and ecotoxicological effects of sweeteners is increasing day by day [5,6]. There are lots of studies related with carcinogenicity, genotoxicity, and toxicity about aspartame [2,7–9]. In recent years, artificial sweeteners from various resources are detected in wastewater, surface water, and groundwater [6]. The presence of these organic compounds in water since most of them are neurotoxic, endocrine disrupting, mutagenic or potentially carcinogenic at very low concentrations [10].

The removal of sweeteners is difficult with conventional treatment plants [11]. Therefore, advanced oxidation

* Corresponding author.

process (AOP) has been used as an effective method to degrade organic pollutants [12–14]. AOPs involve the generation of strong oxidants (hydroxyl radicals), which are highly reactive species. These radicals are able to oxidize pollutants (especially, organic pollutants) and transform them to CO_2. With the addition of hydrogen peroxide (H_2O_2) oxidation, the treatment plants with AOPs, such as ozonation (O_3) or ultraviolet (UV) radiation have shown to transform a broader range of organic pollutants such as artificial sweeteners [15].

Therefore, the removal of such compounds can be achieved by O_3-based AOPs, which combine O_3 with a homogeneous or a heterogeneous catalyst in all producing utilized strong oxidizing species produced in situ such as hydroxyl radicals (•OH) to induce a number of reactions that convert organic compounds into one or more double bonds and smaller and less harmful substances such as CO_2, H_2O, and organic short chain acids [1]. These technologies are of great influence because, in addition to O_3 direct reactions, they contain the action of $HO^{\cdot}$ produced allows different synergies to be discovered [16]. In literature, there are a lot of studies about catalytic ozonation for degradation of organic contaminants via alumina [17], for chlorinated VOCs via ZSM-5 zeolites [18], and alumina and for paracetamol via zeolite [19].

TiO_2 has been widely applied in nanosize forms to provide the higher surface area. However, the challenges related to the separation and recovery of nanosize particles required the exhaustive efforts [20,21]. A number of studies have minimized this problem by coating TiO_2 on a variety of support materials, such as pumice, glass, silica gel, metal, ceramics, polymer, thin films, fibers, zeolite, alumina clays, activated carbon, cellulose, reactor walls, etc. [22].

In this study, the pumice surface was modified with nano-titanium dioxide in order to increase the efficiency of ozonation. The aspartame removal in aqueous solution was investigated by nano-titanium coated pumice (n-TCP)/O_3 process.

To the best of our knowledge, removal of aspartame in aqueous solution has not been studied by catalytic ozonation. Therefore, the aim of the study involves different parts such as: (i) effect of nano-TiO_2 loading on pumice due to structure and surface properties, (ii) contributions from direct/indirect ozonation and surface adsorption effects on aspartame removal, (iii) to examine the synergistic effects of different operational parameters such as different pollutant and catalyst dosages on the heterogeneous catalytic ozonation, and (iv) identification of TBA effect on the performance of catalytic ozonation.

2. Materials and methods

2.1. Catalyst preparation

The natural pumice stone was procured from a Hasan Mountain Area, Aksaray Province, Turkey. These samples were separated into four different particle size fractions with sieve analysis. After that, the raw samples were washed several times with distilled and deionized water (DDW) to purify the impurities until the effluent turbidity reached less than 1 NTU and then dried at 55°C for 72 h. The surface porosity was increased by adding 1 M HCl and dried at 60°C for 24 h. The surface voids of dried pumices were cleaned with acetone solution and dried at 55°C for 24 h. TiO_2 was added by weight of 40% to pumice and six drops of 6 M NaOH solution was added per gram of mixture. This suspension was shaken for 24 h at 200 rpm at a temperature around 60°C. Then the suspension was filtered, followed by washing of pumice several times with DDW and dried at about 70°C for 168 h. After the coating process, the nano-titanium coated pumice (n-TCP) samples were washed several times until the effluent turbidity was reached less than 1 NTU. The washed pumice samples were dried for 36 h at 40°C. The resulting surface-modified pumice was used throughout the study. The chemicals used in the present study are all of analytical grade obtained from Sigma-Aldrich, Israel.

2.2. Materials

TiO_2 anatase (anatase > 99%, crystalline size 10 nm) was purchased from Ege Nanotek Kimya Sanayi (Ege Nanotek Chemical Industry), Turkey. NaOH and H_2SO_4 were purchased from Merck, Turkey. Aspartame was procured from Sigma-Aldrich, Turkey. All the chemicals were used as received without any further purification. All solutions were prepared using ultrapure water from Milli-Q synthesis Unit (Millipore).

2.3. Analyses and experimental procedure

All experiments were carried out in a 1 L borosilicate cylindrical reactor equipped with bubbling and agitation and inlets for measuring temperature, ozone concentration, sampling point. The experimental procedure has been given in detail in a previous study [23]. In all the experiments, at determined intervals, aliquots of samples were withdrawn from the reactor and filtered (0.22 μm microfilter) to retain n-TCP particles and to obtain a clear solution. A certain amount of sodium sulfite solution (0.1 M) was added into the taken aqueous sample to trap the residual ozone.

Aspartame decomposition products were analyzed by means of a Shimadzu QP2010 Plus GC/MS (Tokyo, Japan) and an RTX-624 column (60 m × 0.25 mm, 1.40 μm). The characteristic ions of aspartame decomposition products were shown in Table 1. The oven temperature program was 35°C for 1 min, from 35°C to 215°C at 30°C min^{-1}, and finally 3 min at 215°C. Mass spectroscopy was performed under electron impact (70 eV) from 40 to 350 m z^{-1} (1 scan s^{-1}). Column flow and average velocity values were 2 mL min^{-1} and 31.82 cm s^{-1}, respectively. The interface and transfer lines were maintained at 200°C and 230°C, respectively. The injector was at 250°C and injections (2 μL) were performed in split mode (split ratio 1/120).

Table 1
Retention time and mass spectrometric data for the target compound

Peaks	tR	Molecular weight	Characteristic ions (m z^{-1})
Toluene	7.18	92	91
Ethylbenzene	7.98	106	91
Ethenylbenzene	8.29	104	78

3. Results and discussion

3.1. Catalyst characterization

The SEM micrograph as illustrated in Fig. 1 revealed that the particle size of n-TCP was in the nanometer range. This small particle size provides large surface area for hydroxyl ions (OH^-) of the solution come in contact with the n-TCP surface to form hydroxyl radical, which is a strong oxidizing agent and oxidize a large amount of aspartame molecules adsorbed on the surface of n-TCP. It was also observed from the figure that the particles were spherical shaped, smooth informally distributed and the shape of the catalyst was in homogeneous structure and no odd structures were detected on the surface.

The surface area of raw and nano-TiO_2 coated pumice was determined from desorption isotherms while applying BET-N_2 method. After the coating process, the weight of Ti was 5.55%. After coating with the TiO_2, catalyst surface area expanded (17.445 m^2 g^{-1}) approximately 10 times. Despite this lower surface area of raw pumice compared with n-TCP alone, the highest removal efficiencies were observed with the lowest dosage of n-TCP. This phenomenon can be explained as follows: n-TCP becomes easily oxidized and aggregated due to a higher specific surface area. The point of zero charges of n-TCP and raw pumice was determined by mass titration method [24] and found to be 7.09 and 6.97 (Table 2).

n-TCP enters into a reaction with anionic pollutants within acidic pH ranges due to its neutral pH_{PZC}, thus allowing the pollutant to be adsorbed and/or oxidized. If the pH of the solution is below the pH_{PZC}, the more thicker double layer can be observed because of electrostatic repulsion among the surface and the cations. This situation is limited to the adsorption between the pollutant and the surface.

FT-IR is an analysis method that can give information about the spectra of carboxyl, carbonyl, hydroxyl, amino, and other functional groups, as well as double and triple bonds. FT-IR spectrum of n-TCP showed various characteristic peaks as shown in Fig. 2. When the spectra are compared, the changes in the absorption peaks in the spectra belonging to n-TCP are striking. The strongest adsorption peaks were observed at 3,000 and 3,600 cm^{-1}, which indicates hydroxyl groups. It is considered that this is due to the moisture content of the hydroxyl groups and related to stretching and vibrating of free intermolecular and intramolecular H bonds [25]. FT-IR spectrum of the n-TCP sample shows transmittance peaks in the range 500–1,000 cm^{-1}. This is assigned to the vibrations of Ti–O and Ti–O–Ti framework bonds, which is the characteristic peaks of TiO_2.

3.2. Adsorption of aspartame

The catalytic ozonation is a complex reaction which involves gas, liquid, and solid (three phases) [26]. The solid catalyst may affect the mass transfer of O_3 and its decomposition rate in aqueous solution [27]. The adsorption of ozone and pollutant to generate radicals is an essential step for initiating a favorable catalytic reaction. For this reason, in order to determine the adsorption ability of the catalyst, adsorption capacity was investigated in both different diameters and different pollutant doses. Since adsorption in

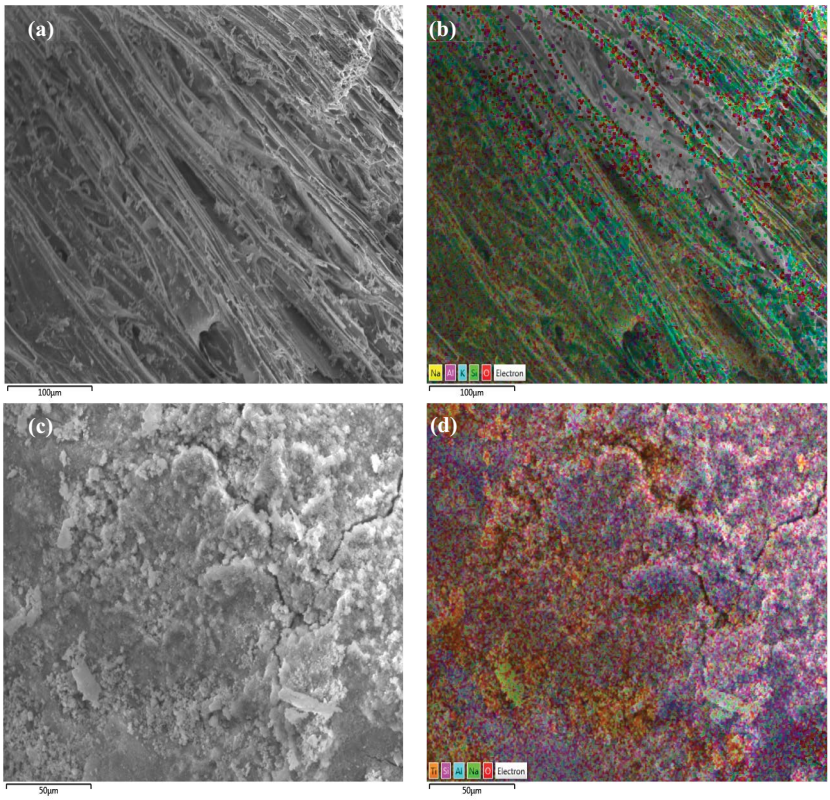

Fig. 1. SEM photograph of the catalyst: ((a) and (b)) raw pumice, and ((c) and (d)) TCP.

Table 2
Physicochemical properties (BET, DLS, and EDX analysis) of raw and nano-TiO_2 coated pumice

Material	Raw pumice	n-TCP
Surface area (m^2 g^{-1})	1.792	17.445
Pore volume (cc g^{-1})	0.008	0.044
Total pore volume (cc g^{-1})	8.582 e^{-03}	6.264 e^{-02}
Weight of Ti (%)	–	5.55
pH_{PZC}	6.97	7.09

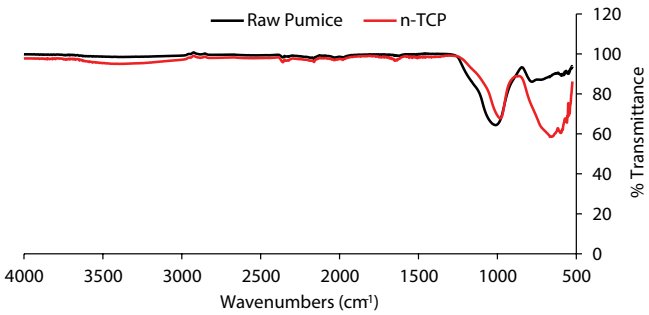

Fig. 2. FT-IR spectrum of raw and nano-TiO_2 coated pumice.

photocatalytic processes can be a crucial step to improve the efficiency of oxidation. However, regardless of the experimental conditions applied, adsorption of aspartame on the n-TCP surface was approximately 20% after 60 min treatment as observed in Figs. 3 and 4. These results indicate that sole adsorption was not good enough to remove the aspartame and the time needed to be extended to 60 min as same as literature [16].

It is thought that the physical adsorption and aspartame removal effect of the catalyst having a size greater than 200 mesh with a surface area of 17.445 m^2 g^{-1} is limited by the restriction of pore volumes. The particle size was confirmed as the significant influence on adsorption in this study. Studies have shown that particle size generally has a strong relationship with adsorption capacity [28,29]. There is an opposite relation between the mesh ratio and the radius of particles. Adsorption study showed that the adsorption capacity increased due to the highest particle capacity (>200 fraction [the smallest particle radius] as same as our study; Fig. 3). As indicated in the literature, the interlayer structure of fine fractions adsorbed more compounds than did coarse fractions [30].

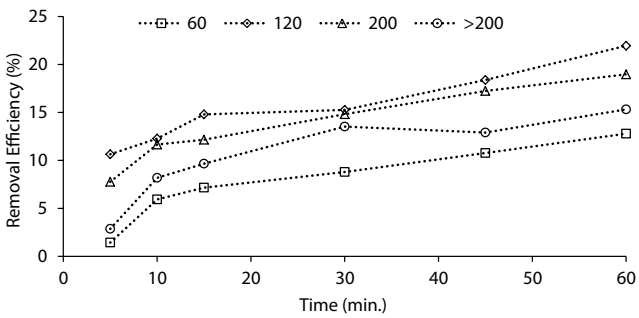

Fig. 3. Adsorption of aspartame at different particle sizes ([Asp.] = 100 μM; [TCP] = 50 mg L^{-1}; pH = 6.9; 600 rpm).

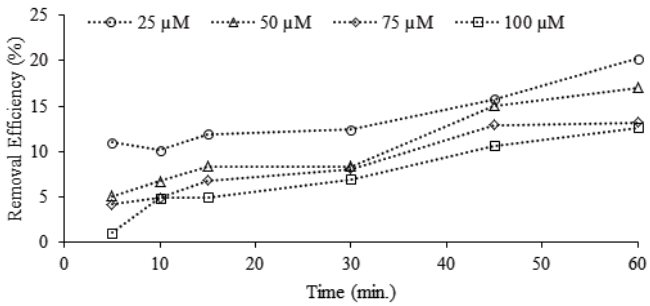

Fig. 4. Adsorption of aspartame at different initial concentrations ([TCP] = 50 mg L^{-1}; pH = 7.1; 600 rpm).

3.3. Sole ozonation of aspartame

In the second series of experiments, ozone was applied by varying its concentration in the gas fed to the reactor. To understand the sole ozonation activity for removal of aspartame, different ozone dosages (6–12 mg L^{-1}) was utilized. Fig. 5 displays the degradation rate of aspartame in sole ozonation processes. After reaction for 60 min, the aspartame removal rate is 25.39% and 30.08% at 10–12 mg L^{-1} ozone dosages. With increasing of ozone dosage, the degradation efficiency increased. Thus, direct ozone cannot effectively remove aspartame as indicated in the literature [31].

3.4. Synergic effect of combined n-TCP/ozonation

Heterogeneous catalysts with higher stability can improve the efficiency of ozone decomposition, and due to these advantages, the heterogeneous catalytic ozonation is used widely in treatment. The most important factor for the heterogeneous catalytic system is the choice of catalysts such as metal oxides, and metals or metal oxides on supports [32]. This mechanism proposes that the metal oxide catalysts can increase the solubility of ozone and initiates the ozone decomposition. Ozone and organic pollutants are adsorbed to the catalyst surface, a series of radical chain transfer occurred to generate much $HO^{\cdot}$, which can oxide the organic pollutants in aqueous media. The percentage degradation of aspartame

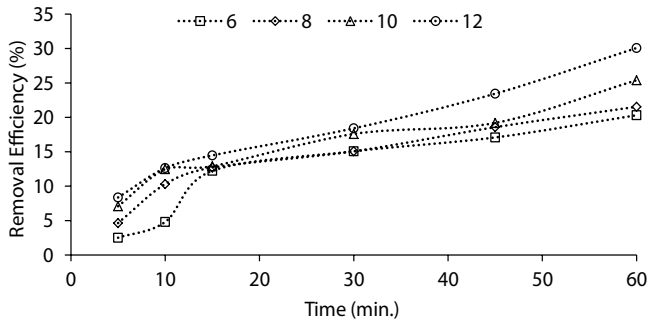

Fig. 5. Sole ozonation of aspartame at different initial ozone concentrations ([Asp.] = 100 μM; pH = 7.1).

increased with the increase of catalyst dosages as depicted in Fig. 6. This is because when the aspartame was allowed to remain in contact with the catalyst for more time, more amount of aspartame adsorbed onto the catalyst surface and consequently, more amount of aspartame was degraded due to the generation of the increased amount of hydroxyl radicals by the catalyst. But after 50 mg L^{-1} catalyst dosage, the increasing aspartame reaction rate was not as high as expected because of competition for degradation between the reactant and the intermediate products formed during degradation. The slow degradation after 50 mg L^{-1} catalyst dosage is due to the slow reaction of short-chain aliphaticentity with hydroxyl radicals and a short lifetime of catalyst because of active sites deactivation by strong by-products deposition [33].

In the final step of experiments, the combination of ozone with catalyst (n-TCP) was utilized for effectively improving the aspartame removal. The presence of n-TCP could improve the mass transfer of ozone and the solubility of ozone in aqueous solution leading to an enhancement of aspartame removal. These results are clearly shown in Figs. 6 and 7. The similar implication was done by some researchers [29,34]. In literature, there was one study about removal of aspartame by advanced oxidation systems. In this study, researchers aimed to remove aspartame by the electrochemical advanced oxidation system. They used a carbon-felt cathode and a Pt or boron-doped diamond (BDD) anode. They found that the optimal conditions are: [Fe] = 0.2 mM, intensity = 200 mA at BDD anode. The removal rate was approximately 100% at 15 min. But electrochemical systems are more difficult to utilize than catalytic ozonation. The results show clearly that the heterogeneous catalytic ozonation system was substantial

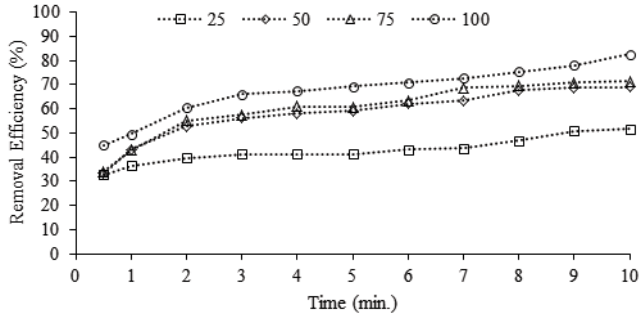

Fig. 6. Catalytic ozonation of aspartame at different catalyst dosages ([O_3] = 10 mg L^{-1}; [Asp.] = 50 μM; pH = 7).

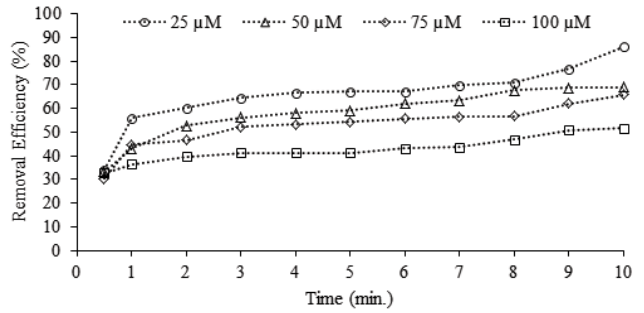

Fig. 7. Catalytic ozonation of aspartame at different initial concentrations ([TCP] = 50 mg L^{-1}; [O_3] = 10 mg L^{-1}; pH = 7.1).

for the removal of aspartame than other advanced oxidation methods.

The obtained apparent rate constant values ($k_{obt.}$) both surface adsorption, sole ozonation, and catalytic ozonation are given in Eqs. (1)–(3).

$$\text{TCP} + \text{aspartame} \rightarrow \text{products}\ k_{ads} : 3.25 \pm 0.05 \times 10^{-8}\,\text{M}^{-1}\text{s}^{-1} \quad (1)$$

$$\text{O}_3 + \text{aspartame} \rightarrow \text{products}\ k_{\text{O}_3} : 6.06 \pm 1.10 \times 10^{-8}\,\text{M}^{-1}\text{s}^{-1} \quad (2)$$

$$\text{TCP/O}_3 + \text{aspartame} \rightarrow \text{products}\ k_{\text{Cat-O}_3} : 1.10 \pm 0.55 \times 10^{-6}\,\text{M}^{-1}\text{s}^{-1} \quad (3)$$

According to the results which are given (Eqs. (1)–(3)), the extent of synergism can be calculated by Eq. (4):

$$\text{A synergisms} = \frac{k_{\text{Cat-O}_3} - \left(k_{ads} + k_{\text{O}_3}\right)}{k_{\text{Cat-O}_3}} \quad (4)$$

where $k_{\text{Cat-O}_3}$, k_{O_3}, and k_{ads} are first-order rate constants corresponding to catalytic ozonation, sole ozonation, and adsorption, respectively. Synergism percentage was calculated to be 91.53% due to Eq. (4). According to synergism, the catalytic ozonation was crucial and combining the adsorption and ozonation gave satisfactory results.

3.5. Radical scavenger effect on heterogeneous catalytic ozonation performance

In the presence of an n-TCP catalyst, aspartame degradation increases due to the formation of some active species (hydroxyl radicals especially) during catalytic ozonation system. The improvement of active species (OH•) formation which causes the enhancement of catalytic ozonation should be examined. Therefore, TBA that was known as a strong organic radical scavenger [35] was used to prove OH• formation in catalytic ozonation. The molecular ozone reaction rate constant was 3.0 × 10^{-3} M^{-1} s^{-1} [36,37], on the other hand the constant of hydroxyl radical of TBA was 6.0 × 10^{8} M^{-1} s^{-1} [38]. Additionally, due to its chemical and physical properties, the repulsion between TBA and catalyst surface, so TBA cannot be adsorbed on the catalyst surface [39,40]. Since TBA reacts with hydroxyl radicals and terminates the chain reactions of radicals and also it reduces the formation of OH• reacting with organic molecules, TBA is a suitable indicator for radical type reactions. As clearly shown in Fig. 8, TBA reacts with free radicals in the catalytic ozonation system.

To determine the molecular ozone and hydroxyl radical contribution to catalytic ozonation, kinetic coefficients were calculated via the presence of TBA.

In catalytic systems, the heterogeneous and homogeneous reactions occur on the catalyst surface and liquid surface, respectively. Based on this scope, the aspartame degradation kinetics fitted the first order degree.

$$\begin{aligned} -\frac{d[\text{Asp.}]}{dt} &= r_{\text{homogeneous}} + r_{\text{heterogeneous}} \\ &= \left(k_{\text{homogeneous}} + k_{\text{heterogeneous}}[\text{TCP}]\right)[\text{Asp.}] \\ &= k_{\text{observation}}[\text{Asp.}] \end{aligned} \quad (5)$$

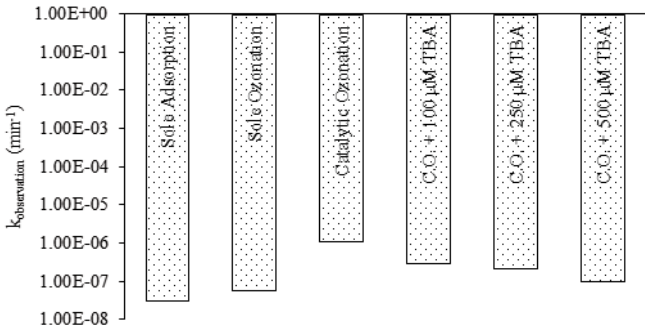

Fig. 8. TBA effect on catalytic ozonation via reaction rate constants ([Asp.] = 50 µM; [TCP] = 50 mg L^{-1}; [O_3] = 10 mg L^{-1}).

$$k_{\text{observation}} = k_{\text{homogeneous}} + k_{\text{heterogeneous}} \tag{6}$$

$$k_{\text{homogeneous}} = k_{O_3}\left[O_3\right] + k_{OH^\bullet}\left[OH^\bullet\right] \tag{7}$$

$$k_{\text{heterogeneous}} = k_{\text{ads}} + k_{\text{ads}-O_3}\left[O_3\right] + k_{\text{ads}-OH^\bullet}\left[OH^\bullet\right] \tag{8}$$

In Eq. (8) [TCP] $k_{\text{observation}}$, k_{O_3}, $k_{OH\bullet}$, k_{ads}, $k_{\text{ads}-O_3}$, and $k_{\text{ads}-OH\bullet}$ terms were explained in other study [26]. Due to the addition of TBA that is known as a radical scavenger, into the reaction chamber, the reaction between the organic pollutant (aspartame) and hydroxyl radical was terminated especially heterogeneous advanced oxidation systems such as catalytic ozonation. The reaction system can be explained basically, first of all ozone adsorbed on TCP surface and the basic reactions about molecular ozone in the liquid phase. The reactions and kinetics of TBA and aspartame can be described by Eq. (9) [41,42] as follows:

$$-\frac{d\left[\text{Asp.}\right]}{dt} = k_{\text{TBA}}\left[\text{Asp.}\right] \tag{9}$$

$$k_{\text{TBA}} = k_{O_3}\left[O_3\right] + k_{\text{ads}} + k_{\text{ads}-O_3}\left[O_3\right]\left[\text{TCP}\right] \tag{10}$$

The OH• fraction ($f_{OH\cdot}$) is calculated by Eq. (11) due to the aspartame consumption and degradation.

$$f_{OH\bullet} = 1 - f_{O_3} = \left(1 - \frac{k_{\text{TBA}}}{k_{\text{total}}}\right) \times \%100 \tag{11}$$

As shown clearly in Figs. 8 and 9, increasing the TBA doses causes the OH• fraction ($f_{OH\cdot}$) to increase. The values vary from 72.2% to 90.5% depending on the increased TBA concentration (Fig. 9). The results show that the predominant species based on the radicals, the hydroxyl radicals (OH•) are predominant in catalytic ozonation systems.

The presence of TBA appears to be clearly evident in its effect on the individual ozonation and catalytic ozonation system, as in other similar studies where it significantly reduces the removal efficiency [43]. The effect of TBA on sole ozonation process only decreases the performance by 13.0%. However, the inhibitory effect of TBA on catalytic ozonation system was more effective. The hydroxyl radicals occur at

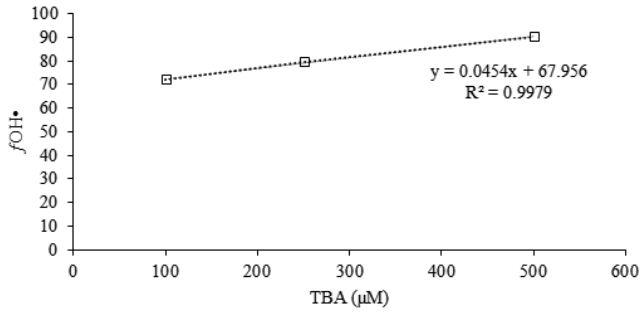

Fig. 9. TBA influence on a hydroxyl radical fraction.

higher amount in catalytic ozonation systems than in the sole ozonation system. Eq. (12) can be written assuming that almost all hydroxyl radicals (OH•) gave reaction at both sole ozonation and catalytic ozonation.

$$k_{\text{observation}-\text{TBA}} = k_{O_3}\left[O_3\right] + k_{\text{ads}}\left[\text{TCP}\right] \tag{12}$$

In this study, adsorption kinetics can be explained by first order kinetic model. Therefore, in adsorption processes:

$$-\frac{d\left[\text{Asp.}\right]}{dt} = k_{\text{ads}}\left[\text{TCP}\right]\left[\text{Asp.}\right] = k_{\text{observation}-\text{adsorption}}\left[\text{Asp.}\right] \tag{13}$$

Aspartame degradation can be explained by three mechanisms as follows: surface adsorption, direct (molecular ozonation), and indirect (OH•) oxidation (Eqs. (14)–(16)).

$$\eta_{\text{ozone}} = 100 - \eta_{OH\bullet} - \eta_{\text{ads}} \tag{14}$$

$$\eta_{OH\bullet} = \left(1 - \frac{k_{\text{observation}-\text{TBA}}}{k_{\text{observation}}}\right) \times \%100 \tag{15}$$

$$\eta_{\text{ads}} = \left(\frac{k_{\text{observation}-\text{ads}}}{k_{\text{observation}}}\right) \times \%100 \tag{16}$$

Based on Eqs. (14)–(16), the contributions of sole adsorption, sole ozonation and catalytic ozonation (η_{ozone}, $\eta_{OH\cdot}$, and $\eta_{\text{adsorption}}$) are calculated (Table 3).

In sole ozonation experiments, the molecular ozone and radicals play a vital role. In contrast, the hydroxyl radicals contribute to the degradation of aspartame catalytic ozonation process (Table 2). The studies were carried out in a neutral pH value so there is no pH adjustment (pH = 7.04). And also, there is no modification in catalyst due to the expensive methods, but the coating procedure is used only as a support surface for the development of reactions.

Table 3
Contribution of oxidation type and adsorption to aspartame degradation

Reaction type	$\eta_{\text{adsorption}}$	$\eta_{OH\cdot}$	η_{ozone}
Sole ozonation	–	5.51	94.49
Catalytic ozonation	2.96	72.20	24.84

4. Conclusions

Removal of aspartame was successfully carried out by combining the n-TCP and ozonation. The physicochemical properties of the newly produced n-TCP catalyst were determined by SEM, EDX, FT-IR, BET, DLS, and pH_{PZC} analyses. All results show that the pumice surface was successfully coated with nano-TiO_2 and a new adhesion surface was formed. There is a limited number of studies on aspartame removal in the literature, so this study will be an important step for other studies. In this study, the adsorption, the sole ozonation, and their synergetic effect (catalytic ozonation) have been studied systematically focusing the degradation of aspartame at different aspartame, ozone, and catalyst dosages. Aspartame removal efficiencies of sole ozonation and sole adsorption were determined as 20.31%–30.08% and 12.62%–21.95% in different operating conditions, respectively. As seen in the results, the singular usage of these systems is insufficient for aspartame removal. The results clearly show that the efficiency of removal is markedly increased by the synergistic effect provided from the combined use of these systems. Synergism percentage was calculated to be 91.53. As it is known, TBA is a radical scavenger used to inhibit the removal efficiency of organic pollutants such as aspartame. Therefore, the OH radical-based mechanism is responsible for the degradation of aspartame by *n*-TCP based catalytic ozonation. The presence of TBA in catalytic ozonation processes inhibited aspartame degradation performance by 72.20%, while this rate remained at 5.51% in sole ozonation processes. Since the formation of $OH^{\bullet}$ radicals in the individual ozonation is less than the catalytic ozonation, the inhibitory effect of TBA, that is, the activity of $OH^{\bullet}$ radicals, is more pronounced in the catalytic ozonation processes. As a result, the efficacy of catalytic ozonation processes in aspartame degradation was proven and the reaction kinetics was calculated as $1.10 \pm 0.55 \times 10^{-6}$ M^{-1} s^{-1}. Furthermore, the effect of n-TCP catalyst used in this study on the degradation of ozone and formation of $OH^{\bullet}$ radical has been determined and has been described as an environmentally friendly catalyst.

Acknowledgments

The authors would like to thank the Environmental Engineering Department of Aksaray University for providing laboratory equipment for the work described in this paper.

References

[1] H. Lin, Removal of Organic Pollutants from Water by Electro-Fenton and Electro-Fenton like Processes, Geophysics, Université Paris-Est, 2015.
[2] A. Otabe, F. Ohta, A. Takumi, B. Lynch, Mutagenicity and genotoxicity studies of aspartame, Regul. Toxicol. Pharm., 103 (2018) 345–351.
[3] K. Xavia, The Dangers of Aspartame, Soil and Health Association, New Zealand, 2013.
[4] W. Giger, Hydrophilic and amphiphilic water pollutants: using advanced analytical methods for classic and emerging contaminants, Anal. Bioanal. Chem., 393 (2009) 37–44.
[5] V.K. Sharma, M. Oturan, H. Kim, Oxidation of artificial sweetener sucralose by advanced oxidation processes: a review, Environ. Sci. Pollut. Res., 21 (2014) 8525–8533.
[6] F.T. Lange, M. Scheurer, H.-J. Brauch, Artificial sweeteners—a recently recognized class of emerging environmental contaminants: a review, Anal. Bioanal. Chem., 403 (2012) 2503–2518.
[7] D. Kirkland, D. Gatehouse, Aspartame: a review of genotoxicity data, Food Chem. Toxicol., 84 (2015) 161–168.
[8] P. Wexler, B.D. Anderson, S.C. Gad, P.B. Hakkinen, M. Kamrin, A. de Peyster, B. Locey, C. Pope, H.M. Mehendale, L.R. Shugart, Encyclopedia of Toxicology, Academic Press, USA, 2005.
[9] L. Haighton, A. Roberts, B. Walters, B. Lynch, Systematic review and evaluation of aspartame carcinogenicity bioassays using quality criteria, Regul. Toxicol. Pharm., 103 (2018) 332–344.
[10] A. Babuponnusami, K. Muthukumar, A review on Fenton and improvements to the Fenton process for wastewater treatment, J. Environ. Chem. Eng., 2 (2014) 557–572.
[11] E.C. Bernardo, T. Fukuta, T. Fujita, E.P. Ona, Y. Kojima, H. Matsuda, Enhancement of saccharin removal from aqueous solution by activated carbon adsorption with ultrasonic treatment, Ultrason. Sonochem., 13 (2006) 13–18.
[12] A. Alver, E. Baştürk, A. Kılıç, M. Karataş, Use of advance oxidation process to improve the biodegradability of olive oil mill effluents, Process Saf. Environ. Prot., 98 (2015) 319–324.
[13] A. Alver, L. Altaş, Characterization and electrocoagulative treatment of landfill leachates: a statistical approach, Process Saf. Environ. Prot., 111 (2017) 102–111.
[14] M.E. Argun, A. Alver, M. Karatas, Optimization of landfill leachate oxidation at extreme conditions and determination of micropollutants removal, Desal. Wat. Treat., 90 (2017) 130–138.
[15] M. Klavarioti, D. Mantzavinos, D. Kassinos, Removal of residual pharmaceuticals from aqueous systems by advanced oxidation processes, Environ. Int., 35 (2009) 402–417.
[16] E.M. Rodríguez, G. Márquez, E.A. León, P.M. Álvarez, A.M. Amat, F.J. Beltrán, Mechanism considerations for photocatalytic oxidation, ozonation and photocatalytic ozonation of some pharmaceutical compounds in water, J. Environ. Manage., 127 (2013) 114–124.
[17] A. Ikhlaq, D.R. Brown, B. Kasprzyk-Hordern, Catalytic ozonation for the removal of organic contaminants in water on alumina, Appl. Catal., B, 165 (2015) 408–418.
[18] A. Ikhlaq, B. Kasprzyk-Hordern, Catalytic ozonation of chlorinated VOCs on ZSM-5 zeolites and alumina: formation of chlorides, Appl. Catal., B, 200 (2017) 274–282.
[19] A. Ikhlaq, S. Waheed, K.S. Joya, M. Kazmi, Catalytic ozonation of paracetamol on zeolite A: non-radical mechanism, Catal. Commun., 112 (2018) 15–20.
[20] M.J. Arlos, R. Liang, M.M. Hatat-Fraile, L.M. Bragg, N.Y. Zhou, M.R. Servos, S.A. Andrews, Photocatalytic decomposition of selected estrogens and their estrogenic activity by UV-LED irradiated TiO_2 immobilized on porous titanium sheets via thermal-chemical oxidation, J. Hazard. Mater., 318 (2016) 541–550.
[21] M.J. Arlos, M.M. Hatat-Fraile, R. Liang, L.M. Bragg, N.Y. Zhou, S.A. Andrews, M.R. Servos, Photocatalytic decomposition of organic micropollutants using immobilized TiO_2 having different isoelectric points, Water Res., 101 (2016) 351–361.
[22] A.Y. Shan, T.I.M. Ghazi, S.A. Rashid, Immobilisation of titanium dioxide onto supporting materials in heterogeneous photocatalysis: a review, Appl. Catal., A, 389 (2010) 1–8.
[23] A. Alver, A. Kılıç, Catalytic ozonation by ıron coated pumice for the degradation of natural organic matters, Catalysts, 8 (2018) 219.
[24] A. Ikhlaq, D.R. Brown, B. Kasprzyk-Hordern, Mechanisms of catalytic ozonation: an investigation into superoxide ion radical and hydrogen peroxide formation during catalytic ozonation on alumina and zeolites in water, Appl. Catal., B, 129 (2013) 437–449.
[25] B.I. Harman, M. Genisoglu, Synthesis and characterization of pumice-supported nZVI for removal of copper from waters, Adv. Mater. Sci. Eng., 2016 (2016) Article ID: 4372136.
[26] G. Gao, J. Shen, W. Chu, Z. Chen, L. Yuan, Mechanism of enhanced diclofenac mineralization by catalytic ozonation over iron silicate-loaded pumice, Sep. Purif. Technol., 173 (2017) 55–62.
[27] H. Yan, P. Lu, Z. Pan, X. Wang, Q. Zhang, L. Li, Ce/SBA-15 as a heterogeneous ozonation catalyst for efficient mineralization of dimethyl phthalate, J. Mol. Catal. A: Chem., 377 (2013) 57–64.

[28] J.L. Sangster, H. Oke, Y. Zhang, S.L. Bartelt-Hunt, The effect of particle size on sorption of estrogens, androgens and progestagens in aquatic sediment, J. Hazard. Mater., 299 (2015) 112–121.
[29] Y. Luo, J. Chen, C. Wu, J. Zhang, J. Tang, J. Shang, Q. Liao, Effect of particle size on adsorption of norfloxacin and tetracycline onto suspended particulate matter in lake, Environ. Pollut., 244 (2019) 549–559.
[30] C.N. Duong, J.S. Ra, D. Schlenk, S.D. Kim, H.K. Choi, S.D. Kim, Sorption of estrogens onto different fractions of sediment and its effect on vitellogenin expression in male Japanese medaka, Arch. Environ. Contam. Toxicol., 59 (2010) 147–156.
[31] Y. Lin, Z. Peng, X. Zhang, Ozonation of estrone, estradiol, diethylstilbestrol in waters, Desalination, 249 (2009) 235–240.
[32] Y. Guo, L. Yang, X. Cheng, X. Wang, The application and reaction mechanism of catalytic ozonation in water treatment, J. Environ. Anal. Toxicol., 2 (2012) 1–7.
[33] M. Al-Amin, S.C. Dey, T.U. Rashid, M. Ashaduzzaman, S.M. Shamsuddin, Solar assisted photocatalytic degradation of reactive azo dyes in presence of anatase titanium dioxide, Int. J. Res. Eng. Technol., 2 (2016) 14–21.
[34] Z. Bai, Q. Yang, J. Wang, Catalytic ozonation of sulfamethazine antibiotics using $Ce_{0.1}$ $Fe_{0.9}$ OOH: catalyst preparation and performance, Chemosphere, 161 (2016) 174–180.
[35] J. Bing, C. Hu, L. Zhang, Enhanced mineralization of pharmaceuticals by surface oxidation over mesoporous γ-Ti-Al_2O_3 suspension with ozone, Appl. Catal., B, 202 (2017) 118–126.
[36] J. Hoigné, H. Bader, Rate constants of reactions of ozone with organic and inorganic compounds in water—I: non-dissociating organic compounds, Water Res., 17 (1983) 173–183.
[37] J. Hoigné, H. Bader, Rate constants of reactions of ozone with organic and inorganic compounds in water—II: dissociating organic compounds, Water Res., 17 (1983) 185–194.
[38] American Water Works Research Foundation, B. Langlais, D.A. Reckhow, D.R. Brink, Ozone in Water Treatment: Application and Engineering, CRC Press LLC, USA, 1991.
[39] B. Halliwell, J.M. Gutteridge, Free Radicals in Biology and Medicine, Oxford University Press, USA, 2015.
[40] U. Von Gunten, Ozonation of drinking water: Part I. Oxidation kinetics and product formation, Water Res., 37 (2003) 1443–1467.
[41] F. Qi, Z. Chen, B. Xu, J. Shen, J. Ma, C. Joll, A. Heitz, Influence of surface texture and acid–base properties on ozone decomposition catalyzed by aluminum (hydroxyl) oxides, Appl. Catal., B, 84 (2008) 684–690.
[42] B. Lan, R. Huang, L. Li, H. Yan, G. Liao, X. Wang, Q. Zhang, Catalytic ozonation of *p*-chlorobenzoic acid in aqueous solution using Fe-MCM-41 as catalyst, Chem. Eng. J., 219 (2013) 346–354.
[43] B. Xu, F. Qi, J. Zhang, H. Li, D. Sun, D. Robert, Z. Chen, Cobalt modified red mud catalytic ozonation for the degradation of bezafibrate in water: catalyst surface properties characterization and reaction mechanism, Chem. Eng. J., 284 (2016) 942–952.